

Structural and electronic properties of Ge-Si, Sn-Si, and Pb-Si dimers on Si(001) from density-functional calculations

Binghai Yan,^{1,2,*} Kota Tomatsu,³ Bing Huang,² Andreia Luisa da Rosa,¹ Gang Zhou,² Bing-Lin Gu,² Wenhui Duan,² Fumio Komori,³ and Thomas Frauenheim¹

¹Bremen Center for Computational Materials Science, Universität Bremen, Am Fallturm 1, 28359 Bremen, Germany

²Department of Physics, Tsinghua University, Beijing 100084, People's Republic of China

³Institute for Solid State Physics, The University of Tokyo, 5-1-5 Kashiwanoha, Kashiwa-shi, Chiba 277-8581, Japan

(Received 11 February 2009; revised manuscript received 30 April 2009; published 26 June 2009)

Using first-principles methods we studied structural and electronic properties of asymmetric heterogeneous X -Si (X =Ge, Sn, and Pb) dimers on the Si(001) surface and their scatterings for the quasi-one-dimensional π^* electrons. The X -Si dimer with impurity atom X at the lower position scatters more strongly the π^* electrons than that with X at the upper position. Calculated scattering potentials can be qualitatively explained by the difference in p -orbital energy between Si and the lower atom of the X -Si dimer. We predict that the amplitude of electronic standing waves changes significantly between the two oppositely buckled X -Si dimers in differential conductance images of scanning tunneling microscopy. This suggests the possibility of fabricating atomic switches to control the conduction of π^* electrons along the dimer row. Our proposed atomic switches could be achieved by flipping the impurity dimers on the Si(001) surface using the method developed in recent experiments [K. Sagisaka *et al.*, Phys. Rev. Lett. **91**, 146103 (2003)]. Finally, we proposed the model for dimer-flipping mechanism, which can explain previous experiment [K. Sagisaka and D. Fujita, Phys. Rev. B **71**, 245319 (2005)].

DOI: 10.1103/PhysRevB.79.235437

PACS number(s): 73.20.Hb, 82.20.Wt, 68.37.Ef

I. INTRODUCTION

Recently an atomic seesaw switch was fabricated by Tomatsu *et al.*¹ by buckled tin(Sn)-germanium(Ge) dimers on the Ge(001) surface. Different from conventional atomic switches (e.g., see Ref. 2), the switching process does not require large mass transport such as atomic diffusion. The buckling orientation of Sn-Ge dimers was reversibly and controllably flipped by a scanning tunneling microscopy (STM). The reflection coefficient of Sn-Ge dimers for quasi-one-dimensional (1D) π^* electrons on the surface is largely changed between the oppositely buckled configurations. The switching mechanism based on impurity scattering was further studied by us using STM and first-principles calculations recently.³ The (001) surface of silicon, as the most common semiconductor in industry, adopts a very similar structure with the Ge(001) surface. Systematical study of the scattering by impurity dimers on the Si(001) surface is crucial to understand profoundly the scattering mechanism, predict experimental results, and explore the possibility to fabricate atomic switches.

Similar to the Ge(001) surface, the topmost atoms form buckled dimers on clean Si(001) surface. Those dimers form a dimer row in the (110) direction and the buckling direction alternates within a row. The dimer rows form two possible periodical arrangements: $c(4 \times 2)$, where the relative buckling orientation of the adjacent dimer rows is out of phase, or $p(2 \times 2)$ if in phase. At about 140 K a $c(4 \times 2)$ structure was observed by STM (Ref. 4–6) and treated as the ground state, which as well has been supported by theoretical calculations.^{7–12} However, recently a $p(2 \times 2)$ structure was resolved at below 40 K (Ref. 13–16), and a phase transition between $c(4 \times 2)$ and $p(2 \times 2)$ could be reversibly manipulated by using STM,^{17,18} in which the buckling orientation of

the dimer row can be reversed by controlling the STM bias voltage. Similar experiments on the phase transition have also been performed on the Ge(001) surface¹⁹ in which Sn-Ge dimers are flipped to realize *On* and *Off* of the atomic switch.¹ The surface electronic states open a gap between the filled (π) and empty (π^*) dangling bond states. The π state energetically overlaps with the bulk bands. But the π^* state stays in the bulk gap, having energy dispersion only along the dimer row, mainly constituted by the p_z orbital of the lower atoms in the dimers. The π^* state therefore serves a quasi-1D system along the dimer row and the π^* electrons are scattered by adatoms or steps on the surface. Accordingly, electronic standing waves are observed around the surface defects in differential conductance (dI/dV) images of STM.^{20–22} On the Ge(001) surface, buckled Sn-Ge impurity dimers are observed by STM after deposition of Sn atoms to the Ge substrate at room temperature. In the dI/dV image at 80 K, a standing wave of π^* electrons was observed¹ around the Sn-Ge dimer with Sn at the lower-atom position, which corresponds to the off state of the switch. However, the standing wave was too weak to be observed around the Sn-Ge dimer with Sn at the upper-atom position, which corresponds to the on state of the switch. For convenience, we define the buckled X -Ge dimer on the Ge(001) surface with X at its lower(upper)-atom position as an “ X -Ge L dimer” (“ X -Ge U dimer”). In the same manner, we define the X -Si dimer on the Si(001) surface with X at its lower(upper)-atom position as an X -Si L dimer (X -Si U dimer). Our calculations³ together with the phase-shift analysis of standing waves in experiments have revealed that the Sn-Ge L dimer forms a larger potential barrier (repulsive) for π^* electrons while the Sn-Ge U dimer forms a smaller barrier. On the other hand, we also found that Si-Ge L and U dimers³ form a small potential well (attractive potential) and a small

potential barrier, respectively. The scattering-potential formation of Si (or Sn)-Ge L dimers was attributed to the difference of p atomic-orbital energy between Si (or Sn) and Ge atoms. According to this p -orbital model, the potential height of the X -Si (X stands for group-IV elements Sn and Pb) L dimer on Si(001) surfaces is expected to be larger than that of the X -Ge L dimer on corresponding Ge(001) surfaces. This is due to the larger energy difference in the p orbital between the host (substrate) and foreign (impurity) atoms on Si(001) surfaces than on Ge(001) surfaces. How the X -Si L dimer forms the scattering potential is therefore very intriguing. The larger scattering potential of the L dimer is also highly desirable for the realization of a better atomic switch. For Si(001) surfaces, Ge-Si mixed dimers at the Si-Si dimer position were formed by depositing Ge onto the Si substrate at room temperature.^{23,24} A number of further experimental and theoretical efforts have been devoted to explore their structural and electronic^{24–28} properties. However, the scattering of π^* electrons by mixed impurity-Si dimers on Si(001) surfaces has never been studied so far.

In this paper, based on the density-functional calculations, we study the structural and electronic properties of X -Si ($X = \text{Ge}, \text{Sn}, \text{and Pb}$) mixed dimers on Si(001) surfaces, focusing on the scattering effect of those impurity dimers on π^* electrons. Structural configurations of impurity dimers as well as their topographic STM images for future STM measurements are calculated. Using a nearly-free-electron model, the scattering potential at impurity dimers is derived from the Kohn-Sham band structures. The potential formation is qualitatively explained by the difference in p -orbital energy between Si and the impurity atom. Based on our calculations, we suggest that it is possible to fabricate atomic switches using Ge-Si, Sn-Si, or Pb-Si asymmetric dimers to switch the conductance of quasi-1D π^* state on the Si(001) surface. The switching process is also discussed.

II. CALCULATIONAL METHOD

Density-functional calculations within the Perdew-Wang generalized gradient approximations (GGA) (Ref. 29) were performed using the Vienna *ab initio* simulation package.³⁰ Core electrons were described by ultrasoft pseudopotentials³¹ and the wave functions were expanded using plane waves with a cutoff of 350 eV. The surface was simulated using a repeated slab model with $(4 \times 1)p(2 \times 2)$ unit cells, having eight atomic layers with the bottom Si layer passivated by H atoms. The vacuum layer between slabs was 9 Å. The bottom two Si layers were fixed and all other atoms were fully relaxed until the forces were less than 0.01 eV/Å. We used 2×4 Monkhorst-Pack \mathbf{k} points during structure relaxation and 5×7 Monkhorst-Pack \mathbf{k} points for electronic-structure calculations after relaxation. Within the Tersoff-Hamann scheme,³² the topographic STM images were simulated for those relaxed surfaces by integrating the charge density between Fermi energy (E_f) and STM bias voltage (V). All calculations were performed using the calculated Si equilibrium lattice constant 5.46 Å. Nudged elastic band³³ optimizations were used to calculate the dimer-flipping barrier.

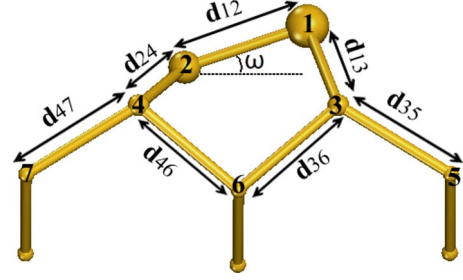


FIG. 1. (Color online) Structure model for a Si-Si dimer on the Si(001) surface viewed from the dimer-row direction. The larger and smaller spheres stand for atoms at higher and lower positions, respectively. We specified atoms using arabic numerals 1–7. Bond lengths, such as d_{12} , and bond angle ω are labeled here.

III. RESULTS AND DISCUSSIONS

Our calculations show that the $p(2 \times 2)$ phase is 1.2 meV per dimer energetically less favorable than the $c(4 \times 2)$ phase, well consistent with previous theoretical work.^{7,8} The relaxed structure of the clean $p(2 \times 2)$ surface with dimer length $A = 2.35$ Å and tilt angle $\omega = 18.6^\circ$ are consistent with previous calculations.^{27,28} When an impurity atom X (Ge, Sn, or Pb) substitutes the lower or upper atom of a Si-Si dimer in the dimer row, the dimer length and the buckling angle change compared to a Si-Si dimer. The side view of a Si-Si dimer is shown in Fig. 1, which indicates the structural parameters listed in Table I. For both X -Si L and U dimers, the dimer length d_{12} is elongated and increases with atomic covalent radius of the X atom. Whereas d_{12} of the X -Si L dimer is a little shorter than that of corresponding U dimer. For X -Si $L(U)$ dimers, the back bond $d_{24}(d_{13})$ connecting the X atom is elongated more with larger X covalent radius. The tilt angle ω decreases (increases) in the order of Ge, Sn, and Pb-Si $L(U)$ dimers. The bond lengths between the second and third layers, d_{36} , d_{46} , d_{35} , and d_{47} , changes around ± 0.01 Å as compared to clean Si(001) surface. The dimer length of neighboring Si-Si dimers to a X -Si dimer is found close to that of the clean surface. Those results indicate that

TABLE I. Bond lengths d_{12} , d_{13} , and d_{24} (Å), and the dimer tilt angle ω (in degrees) for Si-Si dimer on clean Si(001) surface, as defined in Fig. 1. The change in bond lengths and tilt angle, Δd_{12} , Δd_{13} , Δd_{24} , and $\Delta \omega$ for X -Si L and U dimers are shown at the bottom.

Dimer	d_{12}	d_{13}	d_{24}	ω
Si-Si	2.35	2.40	2.34	18.6
Dimer	Δd_{12}	Δd_{13}	Δd_{24}	$\Delta \omega$
Ge-Si L	+0.09	0.00	+0.07	-2.2
Sn-Si L	+0.31	+0.01	+0.26	-6.5
Pb-Si L	+0.42	+0.01	+0.35	-9.5
Ge-Si U	+0.13	+0.10	-0.01	+2.4
Sn-Si U	+0.36	+0.31	-0.01	+5.1
Pb-Si U	+0.47	+0.41	-0.02	+6.1

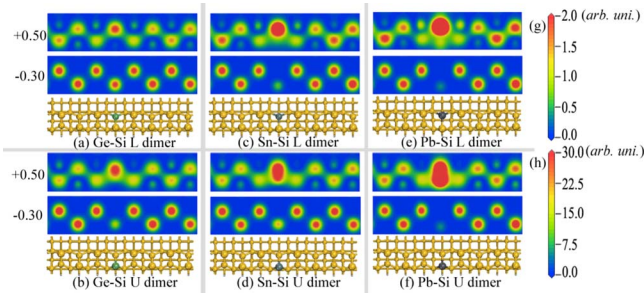


FIG. 2. (Color online) Simulated STM images of a dimer row including Ge-Si (a) L and (b) U dimers, Sn-Si (c) L and (d) U dimers, and Pb-Si (e) L and (f) U dimers for different bias voltage: -0.30 and $+0.50$ eV. The contour plot of integrated charge density is taken on the surface of 2 \AA over the surface top atoms. The color bars for images at (g) $+0.50$ and (h) -0.30 eV are shown on the right, where $1 \text{ a.u.} = 2.15 \times 10^{-4} e/\text{\AA}^3$. Corresponding ball-and-stick structure models viewed from the top are shown at the bottom where yellow balls represent Si atoms and green, gray, and black balls represent Ge, Sn, and Pb atoms, respectively.

the substitution of impurity atoms induces large deformation only for dimer atoms while it does not for deeper layers and neighboring dimers. Energetically, Ge, Sn, and Pb-Si U dimers are 0.15 , 0.25 , and 0.50 eV more stable than corresponding L dimers, respectively. Considering their large atomic radius, X atoms do not prefer the lower position (X -Si L dimer) with compressed stress.³ This is consistent with previous calculations (e.g., see Refs. 26 and 27) for Ge-Si dimers. Furthermore, our calculations revealed that a $p(2 \times 2)$ unit cell with two X -Si U dimers is energetically more stable than that with both an X - X dimer and a Si-Si dimer, by 0.09 , 0.10 , and 0.24 eV for Ge, Sn, and Pb impurities, respectively. It is also consistent with Miwa's calculations²⁶ for the Ge-Si dimer. On the other hand, Ge, Sn, and Pb atoms are found to be energetically more stable at the U -dimer position than at the second atomic layer by 0.37 , 0.73 , and 1.21 eV, respectively. Recent calculations³⁴ also found that there is a large energy barrier for Ge adatoms entering the deeper layer on Si(001) surface. Those results about Ge are consistent with the experimental results that Ge-Si mixed dimers^{23,24} are formed on the Si(001) surface.

Impurity-Si L and U dimers are found to have different bias-voltage (V) dependence of STM images, by which X -Si L and U dimers can be distinguished in experiments. For Sn-Ge L and U dimers on the Ge(001) surface,³ we have simulated their topographic STM images at bias voltages of -0.35 , $+0.35$, and $+0.60$ V, and found good agreement with experimental images at bias voltages of -0.50 , $+0.50$, and $+0.80$ V, respectively. Accordingly we simulated STM images for X -Si dimers on Si(001) at similar bias voltages, -0.30 and $+0.50$ V, as shown in Fig. 2. For Ge-Si dimers [see Figs. 2(a) and 2(b)], the L dimer is imaged as high as Si-Si dimers while the U dimer is imaged lower than Si-Si dimers in filled state image at $V = -0.30$ V. Both Ge-Si L and U dimers are imaged high in empty state images at $V = +0.50$ V and the U dimer looks higher than the L dimer. For Sn-Si dimers [see Figs. 2(c) and 2(d)], both L and U dimers are imaged lower than Si-Si dimers at $V = -0.30$ V and the U

dimer looks relatively higher. For empty state images at $V = +0.50$ V the Sn-Si L dimer is imaged higher than Si-Si dimers but a little lower than the U dimer. For Pb-Si dimers [see Figs. 2(e) and 2(f)], the L dimer is also imaged higher than Si-Si dimers but a little lower than the U dimer for empty state images at $V = +0.50$ V. In addition, Si-Si dimers close to the X -Si dimer are a little lower than another Si-Si dimers in empty images. Those X -Si L and U dimers are imaged as high as Si-Si dimers for filled state images at bias voltage of higher absolute value, e.g., $V = -0.50$ V (not shown here), but much higher than Si-Si dimers for empty state images at bias voltage of higher absolute value, e.g., $V = +0.80$ V (not shown here). It should be pointed out that the calculated bias-voltage value V_b does not quantitatively correspond to the experimental one, especially for empty state images. This is because of the band-gap underestimation in calculation and tip-induced band bending³⁵ in STM experiments.

On the Si(001) surface, the impurity dimer forms a scattering potential $V(x)$ along the dimer row for the quasi-1D π^* electrons. The potential $V(x)$ can be estimated from calculated band structures based on the nearly-free-electron model.³⁶ In the supercell model, the Si dimer row is periodically embedded with impurity dimers that scatter the π^* electron. Therefore the π^* band will split into higher-energy (E_+) and lower-energy (E_-) states at the edge of the first Brillouin zone (FBZ) in the dimer-row direction. Using a nearly-free-electron model, the splitting gap $\Delta E = E_+ - E_-$ is given by

$$\Delta E = 2|V(G)| = 2 \left| \frac{1}{l} \int V(x) e^{iGx} dx \right|, \quad (1)$$

where $G = 2\pi/l$ is the reciprocal lattice vector and l is the distance between two neighboring impurity dimers along the dimer row. For a rectangular potential, $|V(G)|$ is given by

$$|V(G)| = \frac{1}{\pi} |U| |\sin(\pi W/l)|, \quad (2)$$

where $|U|$ is the height or depth of the potential ($U > 0$ and $U < 0$ for the potential barrier and well, respectively) and W is the potential width. On the other hand, as summarized in Ref. 3, the potential type can be obtained by analyzing the charge-density distribution of E_{\pm} state along the dimer row. The charge density of E_+ (E_-) state has a maximum (minimum) in between the X -Si dimers and a minimum (maximum) at the X -Si dimer when the X -Si dimer forms a potential barrier. In contrast, the charge density of E_- (E_+) state has a maximum (minimum) at the X -Si dimers and a minimum (maximum) in between them when the X -Si dimer forms a potential well. The Kohn-Sham band structures for Si(001) surfaces with X -Si dimers are shown in Fig. 3. Larger π^* band-splitting gap ΔE is observed at the FBZ edge for the X -Si L dimer than that for corresponding U dimer, irrespectively of the impurity species. In addition, the 1D characteristic of the π^* state along the dimer row is further confirmed for surfaces with impurity dimers. As an example we show the band structures along $\bar{J}-\bar{\Gamma}-\bar{J}'$ for the Ge-Si L dimer. The π^* band has a very weak dispersion perpendicular to the dimer row ($\bar{J}-\bar{\Gamma}$) and a strong dispersion along the dimer row

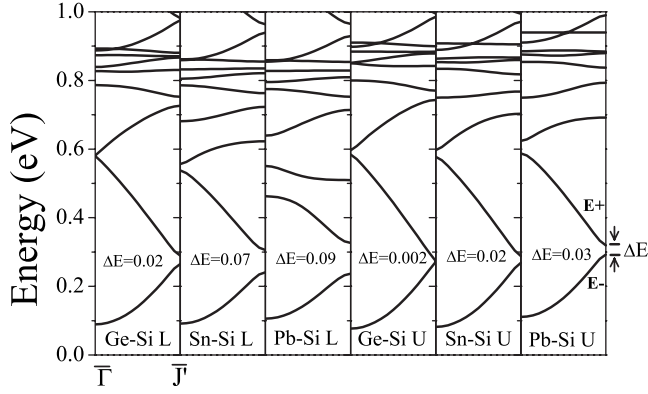


FIG. 3. Calculated Kohn-Sham band structures from $\bar{\Gamma}$ to \bar{J} (dimer-row direction) of Si(001) surfaces with Ge-Si, Sn-Si, and Pb-Si L and U dimers. The Fermi energy is shifted to zero and only the conduction bands are shown with π^* bands at the bottom. Corresponding π^* band splitting ΔE (eV) at \bar{J} are listed.

($\bar{\Gamma}$ - \bar{J}). We adopt the square potential approximation and take the potential width (W) as a dimer length (3.86 Å) for all X -Si dimers. The calculated potential height (depth) $|V(x)| = |U|$ using Eqs. (1) and (2) are shown in Table II as well as the corresponding potential type. Furthermore, the scattering potentials of Pb-Ge L and U dimers on Ge(001) surface were also calculated here and shown in Table II together with previous results for Si and Sn-Ge dimers³ for a systematical study.

Impurity-Si L dimers are found to form a repulsive potential barrier for π^* electrons on Si(001) surface. The barrier height increases in order of Ge, Sn, and Pb. The potential formation can be explained by the relative p -orbital energy (ΔE_p) between X and Si atoms in a 1D tight-binding model. The π^* state is majority dominated by the p_z orbital of the lower atom in a dimer.³⁷ The π^* electron will have different on-site energy, approximated to be the p -orbital energy (E_p) (Ref. 38) of the lower atom at the X -Si dimer. Impurities X (Ge, Sn, and Pb) have higher E_p than that of Si so that they form a potential barrier. Larger difference in E_p (ΔE_p) between X and Si causes larger barrier height. As Table II shows, the potential height of the X -Si L dimer is proportional to corresponding ΔE_p . This mechanism is consistent

with the case of the Ge(001) surface.³ On the Ge(001) surface, the Si-Ge L dimer forms a potential well since the foreign atom Si has lower E_p than the host atom Ge. On the other hand, Sn-Ge and Pb-Ge L dimers form potential barriers since Sn and Pb have higher E_p than Ge. On the other hand, the Ge-Si U dimer is found to form a quite small potential well while Sn and Pb-Si U dimers form several times smaller potential barriers compared to corresponding Sn and Pb-Si L dimers, respectively. This result can qualitatively be explained by the fact that those U dimers have Ge atoms at the lower-atom position and the on-site energy is nearly homogeneous along the dimer row.

The amplitude of the standing waves around the Sn-Ge dimer on the Ge(001) surface is largely changed in the dI/dV images when the dimer is flipped.¹ Based on the results of scattering potentials in Table II, we predict that similar change in wave amplitude by dimer flipping will occur for X -Si dimers on Si(001) surfaces and Pb-Si dimers on Ge(001) surfaces. The atomic switch on the Ge(001) surface¹ used Sn-Ge L and U dimers as off and on states, which were found to form potential barriers of 0.16 and 0.08 eV, respectively. The potential barrier at the X -Si L dimer on Si(001) surface is over three times higher than that at corresponding X -Si U dimer. So it is possible to fabricate atomic switches with considerable on and off ratio using those X -Si L and U dimers. In addition the Pb-Ge L dimer induces a high potential barrier due to the large ΔE_p between Pb and Ge. The Pb-Ge dimer is also a good candidate of the atomic switch.

Recently Sagisaka *et al.*^{17,18} realized the manipulation of Si(001) surfaces between $c(4 \times 2)$ and $p(2 \times 2)$ phases. By controlling the STM bias voltage, they found that the buckling orientation of Si-Si dimer can be reversed. In their experiments the flip-flop motion of dimers will not start until the STM bias voltage is above +0.7 eV. However, the dimer-flipping mechanism is not completely understood. In another work Takagi *et al.*³⁹ proposed a model of the local transformation process from $c(4 \times 2)$ to $p(2 \times 2)$ on Ge(001). We applied this model to investigate the dimer-flipping process on Si(001). First, as Fig. 4 illustrates, the buckling orientation of a dimer on Si(001) (structure 1) changes to form structure 2. Structure 2 has three adjacent dimers with the same buckling orientation and is found to be 0.11 eV higher in energy than perfect surface (structure 1). The dimer-

TABLE II. Band splitting ΔE (eV), calculated scattering-potential height $|U|$ (eV) and type (repulsive barrier or attractive well for π^* electrons), and E_p difference ΔE_p (eV) between the host and foreign atoms for X -Si dimers on Si(001) surfaces and X -Ge dimers on Ge(001) surfaces.

Si(001) surface					Ge(001) surface ^a				
Dimer	ΔE	$ U $	ΔE_p	Type	Dimer	ΔE	$ U $	ΔE_p	Type
Ge-Si L	0.02	0.08	0.09	Barrier	Si-Ge L	0.012	0.05	-0.09	Well
Sn-Si L	0.07	0.29	0.24	Barrier	Sn-Ge L	0.04	0.16	0.15	Barrier
Pb-Si L	0.09	0.37	0.31	Barrier	Pb-Ge L	0.06	0.25	0.22	Barrier
Ge-Si U	0.002	0.01		Well	Si-Ge U	0.012	0.05		Barrier
Sn-Si U	0.02	0.08		Barrier	Sn-Ge U	0.02	0.08		Barrier
Pb-Si U	0.03	0.12		Barrier	Pb-Ge U	0.02	0.08		Barrier

^aResults of Si-Ge and Sn-Ge dimers are taken from Ref. 3.

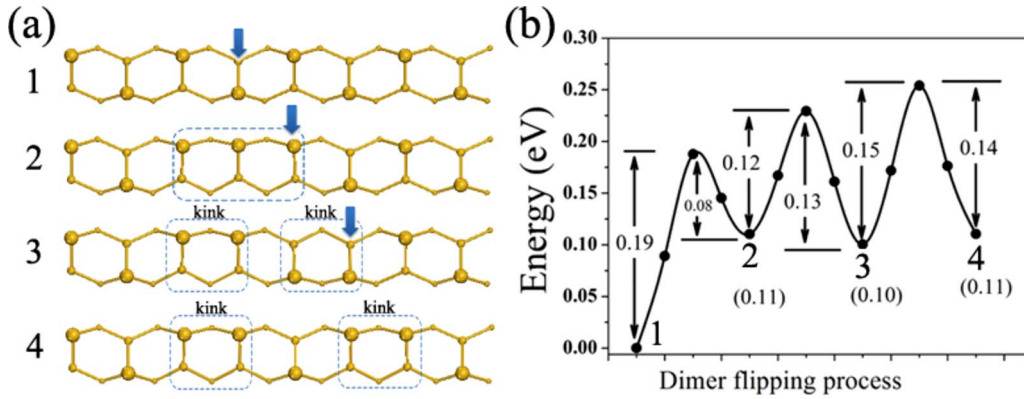


FIG. 4. (Color online) (a) Surface geometries during dimer-flipping process. Structure 1 is a perfect Si(001) dimer row. The arrow indicates the dimer to be flipped. Structure 2 has three adjacent dimers with the same buckling orientation, indicated by the dashed square box. Structure 3 includes two separated kinks and in structure 4 these two kinks move apart. (b) Total-energy change during the dimer-flipping-process structures $1 \leftrightarrow 2 \leftrightarrow 3 \leftrightarrow 4$. The calculated energies are shown by solid circles with the curves as guides for the eyes. The total energy of structure 1 is chosen as zero. Moreover, the relative energies in unit of eV for structures 2, 3, and 4 are shown in corresponding brackets. The barrier height is marked in unit of eV.

flipping barrier from structures 1 to 2 is 0.19 eV. Second, an edge dimer among those three adjacent dimers flips and two separated “kinks” are created (structure 3). Here we called the topological defect having two adjacent dimers of the same buckling orientation as a kink. Structure 3 is found to be 0.10 eV higher in energy than structure 1, which is consistent with previous total-energy calculations.⁴⁰ The flipping barrier in this case is 0.12 eV from structures 2 to 3. Finally, a dimer of the kink flips and the kink moves along the dimer row (structure 4). The dimer-flipping barrier in this case is 0.15 eV. When these two kinks move apart to the end of the dimer row, the buckling orientation of all dimers in this dimer row is reversed. In this process from structures 1 to 4, the dimer flips one after one and the highest flipping barrier is 0.19 eV. Hwang⁴⁰ even proposed a model in which two neighboring dimers flip at a time. However, in his paper the flipping barrier obtained within local-density approximation GGA is much higher, 0.41 (0.55) eV (the total-energy variation shown in Ref. 40 should be multiplied by the dimer number 4 to directly compare with our result). Our recent work⁴¹ shows that on Ge(001) the dimer flipping is caused by a resonant scattering of the π^* electrons with localized electronic states at the kink. The kink starts to move when the π^* -electron energy is higher than a threshold energy, which is determined by the localized-state energy. Recent Monte Carlo simulations⁴² suggested that on Si(001) the kink defect markedly affects the phase transition, which involves the dimer flipping. So we expect that Si(001) has a similar mechanism for dimer flipping in a kink. To further verify that, we have calculated the electronic structure of a Si(001) surface with a kink using a supercell including 11 dimers along the dimer row. We also found a localized state at the kink position among empty states. It overlaps energetically with the π^* state and is 0.80 eV above the Fermi energy.⁴³ Then the bias-voltage threshold in the experiment of Sagisaka *et al.* can be directly correlated with the energy of the

localized state at the kink. Further experiments are required to verify our proposed model for dimer flipping on the Si(001) surface.

IV. CONCLUSION

In conclusion, we studied the structural and electronic properties of impurity X (Ge, Sn, and Pb)-Si dimers on Si(001) surfaces. These asymmetric dimers have been found to be energetically stable. We simulated their topographic images for future STM observation. Compared to corresponding X-Si U dimer, the X-Si L dimer induces stronger scattering for π^* electrons along the dimer row. This can be attributed to the energy difference in the p orbital between the lower atom of the impurity dimer and the Si atom. The scattering-potential height and potential type were estimated from the calculated electronic structure with the aid of a nearly-free-electron model. Impurity-Si dimers can work as atomic switches by reversing their buckling orientation, which might be realized using the recently developed method to manipulate the Si-Si dimer buckling direction reversibly.^{17,18} We propose that it is possible to realize atomic switches with better on/off scattering ratio using X-Si dimers on the Si(001) surface or Pb-Ge dimers on the Ge(001) surface. The switching mechanism related to dimer flipping is also discussed. The energy barriers of a possible dimer-flipping model involving kink creation and motion are calculated. The energy of the localized state at the kink position could explain previous STM experiment of Sagisaka *et al.*¹⁸ by the resonant scattering of the π^* electrons.

ACKNOWLEDGMENTS

The authors thank K. Wu and C. Liu for their valuable discussions. B.Y. acknowledges financial support by the Alexander von Humboldt Foundation of Germany. This work has been partially supported by JSPS-NSFC-KOSEF and A3 Foresight Program.

*bhyan@bccms.uni-bremen.de

- ¹K. Tomatsu, K. Nakatsuji, T. Iimori, Y. Takagi, H. Kusunohara, A. Ishii, and F. Komori, *Science* **315**, 1696 (2007).
- ²K. Terabe, T. Hasegawa, T. Nakayama, and M. Aono, *Nature (London)* **433**, 47 (2005); F.-Q. Xie, L. Nittler, Ch. Obermaier, and Th. Schimmel, *Phys. Rev. Lett.* **93**, 128303 (2004); C. P. Collier, E. W. Wong, M. Belohradský, F. M. Raymo, J. F. Stoddart, P. J. Kuekes, R. S. Williams, and J. R. Heath, *Science* **285**, 391 (1999).
- ³K. Tomatsu, M. Yamada, K. Nakatsuji, F. Komori, B. Yan, C. Wang, G. Zhou, and W. Duan, *Phys. Rev. B* **78**, 081401(R) (2008).
- ⁴H. Tochihara, T. Amakusa, and M. Iwatsuki, *Phys. Rev. B* **50**, 12262 (1994).
- ⁵K. Hata, S. Yasuda, and H. Shigekawa, *Phys. Rev. B* **60**, 8164 (1999).
- ⁶T. Mitsui and K. Takayanagi, *Phys. Rev. B* **62**, R16251 (2000).
- ⁷J. Ihm, D. H. Lee, J. D. Joannopoulos, and J. J. Xiong, *Phys. Rev. Lett.* **51**, 1872 (1983).
- ⁸A. Ramstad, G. Brocks, and P. J. Kelly, *Phys. Rev. B* **51**, 14504 (1995).
- ⁹J. Fritsch and P. Pavone, *Surf. Sci.* **344**, 159 (1995).
- ¹⁰A. A. Stekolnikov, J. Furthmüller, and F. Bechstedt, *Phys. Rev. B* **65**, 115318 (2002).
- ¹¹D. Riedel, M. Lastapis, M. Martin, and G. Dujardin, *Phys. Rev. B* **69**, 121301(R) (2004).
- ¹²K. Inoue, Y. Morikawa, K. Terakura, and M. Nakayama, *Phys. Rev. B* **49**, 14774 (1994).
- ¹³K. Hata, S. Yoshida, and H. Shigekawa, *Phys. Rev. Lett.* **89**, 286104 (2002).
- ¹⁴S. Yoshida, T. Kimura, O. Takeuchi, K. Hata, H. Oigawa, T. Nagamura, H. Sakama, and H. Shigekawa, *Phys. Rev. B* **70**, 235411 (2004).
- ¹⁵K. Sagisaka, M. Kitahara, and D. Fujita, *Jpn. J. Appl. Phys.* **42**, L126 (2003).
- ¹⁶T. Uozumi, Y. Tomiyoshi, N. Suehira, Y. Sugawara, and S. Morita, *Appl. Surf. Sci.* **188**, 279 (2002).
- ¹⁷K. Sagisaka, D. Fujita, and G. Kido, *Phys. Rev. Lett.* **91**, 146103 (2003).
- ¹⁸K. Sagisaka and D. Fujita, *Phys. Rev. B* **71**, 245319 (2005).
- ¹⁹Y. Takagi, Y. Yoshimoto, K. Nakatsuji, and F. Komori, *J. Phys. Soc. Jpn.* **72**, 2425 (2003).
- ²⁰T. Yokoyama, M. Okamoto, and K. Takayanagi, *Phys. Rev. Lett.* **81**, 3423 (1998).
- ²¹K. Sagisaka and D. Fujita, *Appl. Phys. Lett.* **88**, 203118 (2006).
- ²²K. Sagisaka and D. Fujita, *Phys. Rev. B* **72**, 235327 (2005).
- ²³L. Patthey, E. L. Bullock, T. Abukawa, S. Kono, and L. S. O. Johansson, *Phys. Rev. Lett.* **75**, 2538 (1995).
- ²⁴X. Chen, D. K. Saldin, E. L. Bullock, L. Patthey, L. S. O. Johansson, J. Tani, T. Abukawa, and S. Kono, *Phys. Rev. B* **55**, R7319 (1997).
- ²⁵S. J. Jenkins and G. P. Srivastava, *Surf. Sci.* **377-379**, 887 (1997).
- ²⁶R. H. Miwa, *Surf. Sci.* **418**, 55 (1998).
- ²⁷S. C. A. Gay and G. P. Srivastava, *Phys. Rev. B* **60**, 1488 (1999).
- ²⁸K. Seino, W. G. Schmidt, and F. Bechstedt, *Phys. Rev. Lett.* **93**, 036101 (2004).
- ²⁹J. P. Perdew, J. A. Chevary, S. H. Vosko, K. A. Jackson, M. R. Pederson, D. J. Singh, and C. Fiolhais, *Phys. Rev. B* **46**, 6671 (1992).
- ³⁰G. Kresse and J. Hafner, *Phys. Rev. B* **47**, 558(R) (1993); G. Kresse and J. Furthmüller, *ibid.* **54**, 11169 (1996).
- ³¹D. Vanderbilt, *Phys. Rev. B* **41**, 7892 (1990).
- ³²J. Tersoff and D. R. Hamann, *Phys. Rev. B* **31**, 805 (1985).
- ³³G. Henkelman, B. P. Uberuaga, and H. Jónsson, *J. Chem. Phys.* **113**, 9901 (2000).
- ³⁴F. Zipoli, S. Cereda, M. Ceriotti, M. Bernasconi, Leo Miglio, and F. Montalenti, *Appl. Phys. Lett.* **92**, 191908 (2008).
- ³⁵M. McEllistrem, G. Haase, D. Chen, and R. J. Hamers, *Phys. Rev. Lett.* **70**, 2471 (1993).
- ³⁶H. Ibach and H. Lüth, *Solid-State Physics: An Introduction to Principles of Materials Science* (Springer-Verlag, Berlin, 1995).
- ³⁷H. Ibach, *Physics of Surfaces and Interfaces* (Springer, New York, 2006).
- ³⁸S. Kotochigova, Z. H. Levine, E. L. Shirley, M. D. Stiles, and C. W. Clark, *Atomic Reference Data for Electronic Structure Calculations, Version 1.4* (National Institute of Standards and Technology, Gaithersburg, MD, 2005).
- ³⁹Y. Takagi, Y. Yoshimoto, K. Nakatsuji, and F. Komori, *Surf. Sci.* **559**, 1 (2004).
- ⁴⁰G. S. Hwang, *Surf. Sci.* **465**, L789 (2000).
- ⁴¹K. Tomatsu, B. Yan, M. Yamada, Y. Takagi, G. Zhou, W. Duan, and F. Komori, *Surf. Sci.* **603**, 781 (2009).
- ⁴²H. Kawai, O. Narikiyo, and K. Matsufuji, *J. Phys. Soc. Jpn.* **76**, 034602 (2007).
- ⁴³Here the valence top of the bulk silicon is adopted as the Fermi energy of the surface.